THE JOURNAL OF BIOLOGICAL CHEMISTRY VOL. 287, NO. 20, pp. 16849–16859, May 11, 2012

Phospholipase A_2IVα Regulates Phagocytosis Independent of Its Enzymatic Activity*[S]

Received for publication, September 30, 2011, and in revised form, February 24, 2012 Published, JBC Papers in Press, March 5, 2012, DOI 10.1074/jbc.M111.309419

Pasquale Zizza[‡¶1], Cristiano Iurisci[¶], Matteo Bonazzi[‖2], Pascale Cossart[‖], Christina C. Leslie[**], Daniela Corda[‡¶3], and Stefania Mariggiò[‡¶4]

From the [‡]Institute of Protein Biochemistry, National Research Council, Via Pietro Castellino 111, 80131 Naples, Italy, the [¶]Department of Cell Biology and Oncology, Consorzio Mario Negri Sud, Via Nazionale, 66030 Santa Maria Imbaro, Chieti, Italy, the [‖]Unité des Interactions Bactéries-Cellules, INSERM U604, Institut Pasteur, 25 Rue du Dr. Roux, 75724 Paris, France, and the [**]Department of Pediatrics, National Jewish Health, Denver, Colorado 80206

Background: The mechanistic regulation of phagocytosis by phospholipase A_2 (PLA_2) remains to be defined.
Results: A specific PLA_2 isoform is activated during phagocytosis, translocates to the plasma membrane, and directly participates in phagosome formation, without involving its enzymatic activity.
Conclusion: PLA_2IVα regulates phagocytosis via a novel mechanism that requires membrane binding of its C2 domain.
Significance: PLA_2IVα mediates a novel mechanism of phagocytosis regulation.

Group IVα phospholipase A_2 (PLA_2IVα) is a lipolytic enzyme that catalyzes the hydrolysis of membrane phospholipids to generate precursors of potent inflammatory lipid mediators. Here, the role of PLA_2IVα in Fc receptor (FcR)-mediated phagocytosis was investigated, demonstrating that PLA_2IVα is selectively activated upon FcR-mediated phagocytosis in macrophages and that it rapidly translocates to the site of the nascent phagosome. Moreover, pharmacological inhibition of PLA_2IVα by pyrrophenone reduces particle internalization by up to 50%. In parallel, fibroblasts from PLA_2IVα knock-out mice overexpressing FcγRIIA and able to internalize IgG-opsonized beads show 50% lower phagocytosis, compared with wild-type cells, and transfection of PLA_2IVα fully recovers this impaired function. Interestingly, transfection of the catalytically inactive deleted PLA_2IVα mutant (PLA_2IVα(1–525)) and point mutant (PLA_2IVα-S228C) also promotes recovery of this impaired function. Finally, transfection of the PLA_2IVα C2 domain (which is directly involved in PLA_2IVα membrane binding), but not of PLA_2IVα-D43N (which cannot bind to membranes), rescues FcR-mediated phagocytosis. These data unveil a new mechanism of action for PLA_2IVα, which demonstrates that the membrane binding, and not the enzymatic activity, is required for PLA_2IVα modulation of FcR-mediated phagocytosis.

The phospholipases A_2 (PLA_2s)[5] are lipolytic enzymes that catalyze hydrolysis of the *sn*-2 acyl bond of membrane phospholipids to generate free fatty acids and lysophospholipids (1, 2). As the fatty acids released include arachidonic acid, PLA_2 has a critical role during immune responses through generation of the precursors of the eicosanoids, including the leukotrienes, prostaglandins, and thromboxanes, which are potent inflammatory mediators (3, 4). At the same time, PLA_2 generates lysolipids as the ether-linked lysophospholipids, which are precursors of the inflammatory mediator platelet-activating factor.

The PLA_2 family includes several relatively unrelated proteins, among which are the following: the low molecular weight secreted enzymes (sPLA_2s), which have been implicated in eicosanoid generation, inflammation, host defense, and atherosclerosis (5); the cytosolic Ca^{2+}-independent group VI PLA_2s, which have been reported to have roles in phospholipid homeostasis and membrane remodeling (6); and the group IV cytosolic PLA_2s, which include six high molecular mass enzymes in *Mus musculus* (as PLA_2IVα to PLA_2IVζ), with three newly cloned isoforms (7). PLA_2IVα has an essential role in initiation of the arachidonate pathway, and it is mainly involved in inflammation, intestinal ulceration, acute lung injury, anaphylaxis, and parturition, as shown through the PLA_2IVα knock-out mouse approach (8–10).

PLA_2IVα activity requires up to micromolar concentrations of intracellular Ca^{2+} to promote the binding of two calcium ions to its N-terminal C2 domain, thus inducing a conformational change and translocation of PLA_2IVα from the cytosol to

* This work was supported, in whole or in part, by National Institutes of Health Grants HL34303 and HL61378 (to C. C. L.). This work was also supported by Italian Association for Cancer Research Grant IG10341 (Milan, Italy) (to D. C.), Telethon Italia Grant GGP030295, MIUR (Italy), the European Community Seventh Framework Programme FP7/2007-2013, Grants 202272 HEALTH-2007-2.1.1-6 (LipidomicNet) (to D. C.), and the Italian Ministry of Economy and Finance to the National Research Council (FaReBio di Qualità) (to D. C.).
[S] This article contains supplemental Movies S1–S6.
[1] Recipient of an Italian Foundation for Cancer Research Fellowship (Milan, Italy).
[2] Present address: CNRS, UMR 5236, CPBS, CNRS, 34293 Montpellier, France.
[3] To whom correspondence may be addressed: Institute of Protein Biochemistry, National Research Council, Via Pietro Castellino 111, 80131 Naples, Italy. Tel.: 39-081-6132536; Fax: 39-081-6132277; E-mail: d.corda@ibp.cnr.it.
[4] To whom correspondence may be addressed: Institute of Protein Biochemistry, National Research Council, Via Pietro Castellino 111, 80131 Naples, Italy. Tel.: 39-081-6132578; Fax: 39-081-6132277; E-mail: s.mariggio@ibp.cnr.it.

[5] The abbreviations used are: PLA_2, phospholipase A_2; FcR, Fc receptor; GroPIns, glycerophosphoinositol; GroPIns4*P*, glycerophosphoinositol 4-phosphate; IMLF, immortalized mouse lung fibroblast; lyso-PtdIns, lysophosphatidylinositol; sPLA2, secreted PLA_2; BAPTA-AM, 1,2-bis(2-aminophenoxy)ethane-*N*,*N*,*N*′,*N*′-tetraacetic acid tetrakis(acetoxymethyl ester).

the cell membranes, where it can then access its substrates (11). The initial theory of PLA$_2$IVα membrane translocation was based on hydrophobic interactions of its C2 domain with phosphatidylcholine-enriched membranes in response to an intracellular Ca^{2+} increase (12). However, this has been revised through more recent studies that have shown that the cationic β-groove of the C2 domain can bind to ceramide 1-phosphate on internal membranes (13). Furthermore, the cationic cluster of the PLA$_2$IVα catalytic domain (Lys-488, Lys-541, Lys-543, and Lys-544) can bind to anionic phospholipids, although the requirement for this interaction for membrane translocation or regulation of enzymatic activity is still under debate (14, 15). The majority of these studies have documented translocation of PLA$_2$IVα to internal cell membranes, such as the nuclear envelope, Golgi complex, and endoplasmic reticulum, whereby PLA$_2$IVα contributes to the structure and function of these cell compartments (16–18). Reports have also shown PLA$_2$IVα translocation to the plasma membrane (19, 20).

The role of the phosphorylation of PLA$_2$IVα in induction of membrane translocation is not fully defined, although a requirement for PLA$_2$IVα phosphorylation for its full enzymatic activation has been reported by different groups (15, 21, 22). Serine phosphorylation on PLA$_2$IVα (Ser-505 or Ser-727) is mediated mainly by the mitogen-activated protein kinases (MAPKs) ERK1/2, and by the stress kinases p38 and JNK, and this has been shown to increase the intrinsic enzymatic activity of PLA$_2$IVα (23, 24).

In addition, although phosphatidylcholine is generally considered to be the PLA$_2$IVα substrate (25), the activity of PLA$_2$IVα does not show selectivity for the polar head group of any specific phospholipid substrate, with the only requirement being arachidonic acid in the *sn*-2 position (26). Indeed, PLA$_2$IVα has been shown to be the specific enzyme that produces glycerophosphoinositols from the membrane phosphoinositides upon hormonal stimulation and oncogenic transformation (24, 27, 28).

The PLA$_2$s have been reported to participate in immune cell functions also through the regulation of phagocytosis, as initiated by interactions of ligand-coated particles (particles opsonized with immunoglobulins or complement) with specific receptors expressed on the surface of phagocytic cells (Fc receptors (FcRs) or complement receptors) (29). Phagocytosis induces recruitment of a variety of signaling enzymes and adaptor proteins to the site of particle ingestion, thus resulting in a multifactorial process that triggers the reorganization of the actin cytoskeleton and internalization of the bound particles (30). Moreover, as well as PLA$_2$ involvement, the signaling pathway activated during phagocytosis varies according to cell type, the nature of the stimulus, the number and type of receptors involved, and the ability of certain microorganisms to subvert the phagocytic process (19, 31–35).

Here, we demonstrate that among the early events of macrophage activation triggered by FcR-mediated phagocytosis, there is the selective activation of PLA$_2$IVα, which is shown to translocate to the site of nascent phagosomes and to participate directly in the modulation of the phagocytic process, independent of its enzymatic activity.

EXPERIMENTAL PROCEDURES

Reagents, Antibodies, and Constructs—Bromoenol lactone, lysophosphatidylinositol (lyso-PtdIns), arachidonic acid, REV5901, prostaglandins PGE$_1$ and PGE$_2$, thromboxane B$_2$, leukotrienes (LTB$_4$, LTC$_4$, LTD$_4$, and LTE$_4$), lysopolysaccharides from *Escherichia coli* 055:B5, and 3-μm latex beads were from Sigma. Goat anti-rabbit and anti-mouse IgG horseradish peroxidase conjugates, SB203580, ketoconazole, LY83583, NS398, and sPLA$_2$IIA inhibitor-I were from Calbiochem. Acetylsalicylic acid was from Sinofi Synthelabo (Milan, Italy). U0126 was from Promega (Madison, WI). *myo*-[^{3}H]Inositol (16 Ci/mmol), [5,6,8,9,11,12,14,15-^{3}H]arachidonic acid (210 Ci/mmol), and ECL were from Amersham Biosciences. All of the restriction enzymes were from New England Biolabs (Hitchin, UK). pEGFP-C1 was from Clontech.

Human FcγRIIA was provided by Dr. E. Caron (Imperial College London, London, UK); PLA$_2$IVα in pBK-CMV was from Dr. I. Kudo (Showa University, Tokyo, Japan) (36); GFP-PLA$_2$IVα from Dr. T. Hirabayashi (The Tokyo Metropolitan Institute of Medical Science, Tokyo, Japan); and the GFP-PLA$_2$IVα C2 domain and GFP-PLA$_2$IVα-D43N from Dr. R. L. Williams (Medical Research Council, Cambridge, UK) (12). The GFP-PLA$_2$IVα-S228C construct was obtained by subcloning the 326-bp PmlI-EcoRV fragment from PLA$_2$IVα-S228C (in the pSG5 vector from Dr. B. P. Kennedy, Merck Frosst Centre for Therapeutic Research, Kirkland, Quebec, Canada) into GFP-PLA$_2$IVα (in pEGFP-C1) previously digested with the same enzymes. For the GFP-PLA$_2$IVα(1–525) construct, the 1575-bp BglII-PvuII insert from GFP-PLA$_2$IVα in pEGFP-C1 was subcloned into the pEGFP-C1 vector previously digested with BglII and XmaI. All of the PLA$_2$IVα constructs were of human origin.

The polyclonal anti-PLA$_2$IVα antibody and the preimmune rabbit IgGs were produced according to standard protocols (37). The rabbit polyclonal anti-ERK1 (K-23) and the rabbit anti-phospho-PLA$_2$ (S505) antibodies were from Santa Cruz Biotechnology (San Diego, CA); the 12D4 mouse monoclonal anti-phospho-MAPKs (ERK1/2) clone was from Upstate Biotechnology, Inc. (Lake Placid, NY); the mouse monoclonal anti-phospho-SAPK/JNK (Thr-183/Tyr-185) antibody (G9), the rabbit monoclonal SAPK/JNK antibody (56G8), the rabbit polyclonal anti-phospho-p38 MAPK antibody (Thr-180/Tyr-182), and the rabbit polyclonal anti-p38 antibody were from Cell Signaling Technology, Inc. (Beverly, MA). The mouse monoclonal anti-FcγRIIA antibody (CD32) was from Peliclusster (Amsterdam, The Netherlands). Goat polyclonal HRP-conjugated anti-rabbit and anti-mouse antibodies were from Calbiochem. Alexa568-, Alexa546-, and Alexa488-conjugated anti-rabbit IgGs and Texas Red-zymosan A BioParticle conjugates from *Saccharomyces cerevisiae* were from Molecular Probes, Inc. (Eugene, OR).

Glycerophosphoinositol (GroPIns) and GroPIns 4-phosphate (GroPIns4*P*) were from Echelon Biosciences (Salt Lake City, UT). Pyrrophenone was generously provided by Dr. K. Seno (Shionogi Research Laboratories, Shionogi & Co. Ltd., Osaka, Japan) (38). All other reagents were obtained at the highest purities available from Invitrogen.

Cell Transfection and Immunoblotting—Immortalized mouse lung fibroblasts (IMLFs) (39) were transfected with the Lipofectamine-PLUS reagent (Invitrogen), according to the manufacturer's instructions. To evaluate the overexpression of GFP-tagged PLA_2 mutants in IMLF cells, 100 μg of total cell lysates were blotted with an anti-GFP antibody (Abcam, Cambridge, UK). The activation status of ERK1/2, p38, and JNK was determined as described previously (40). For $PLA_2IV\alpha$ quantification, total cell lysates together with the recombinant $PLA_2IV\alpha$ protein purified from SF9 cells (for methods, see Ref. 24) were blotted with an anti-$PLA_2IV\alpha$ antibody.

Arachidonic Acid and GroPIns Analyses—These procedures were performed as reported in Refs. 40–42.

For stimulation by FcR-mediated phagocytosis, after overnight labeling, the cells were incubated for a further 2 h in serum-free DMEM plus 0.25 μCi/ml [^{3}H]arachidonic acid or 10 μCi/ml *myo*-[^{3}H]inositol, then washed twice, and incubated for 30 min at 4 °C, without or with RIgG-opsonized latex beads, before transfer to 37 °C for the 30-min phagocytosis step. In unstimulated cells, across the full experimental data, the total [^{3}H]arachidonic acid-containing lipid levels were 321,319 ± 43,723 cpm/well for the phagocytosis and 221,558 ± 24,525 cpm/well for LPS stimulation.

The amounts of [^{3}H]GroPIns were expressed as percentages of the total water-soluble cellular radioactivity (42), and in unstimulated cells, the total [^{3}H]inositol-containing aqueous compounds were 43,762 ± 7,774 cpm/well for the phagocytosis, and 72,994 ± 19,132 cpm/well for LPS stimulation.

Phagocytosis Assay—Three μm latex beads were opsonized with 1 mg/ml rabbit IgG for 2 h at 37 °C in phosphate-buffered saline (PBS) and then with 5 ng of Alexa546- or Alexa488-conjugated anti-rabbit IgGs for a further 1 h; excess IgGs were extensively washed out with PBS, and the beads were resuspended in DMEM.

The cells were serum-starved for 2 h and preincubated or not for 15 min with the inhibitors. The opsonized beads (100 beads/cell) or Texas Red-zymosan A particles (100 particles/cell) were then added to the cells, incubated for 30 min at 4 °C, washed with PBS, and incubated in DMEM at 37 °C. Time course experiments of phagocytosis demonstrated that the plateau is reached after 60 min, and 30 min was used in all of the experiments shown. BAPTA-AM addition started 5 min before the incubation at 37 °C to avoid cell detachment.

Phagocytosis was measured by two separate assays. For the morphological analysis, upon completion of phagocytosis the cells were fixed with 4% paraformaldehyde, washed twice in PBS, and permeabilized with 0.5% BSA, 50 mM NH_4Cl, 0.05% saponin in PBS, pH 7.4, and incubated with 0.1% trypan blue. The trypan blue was allowed to freely diffuse into the cells and to counter-stain the internalized beads (visualized only by phase-contrast microscopy), so after trypan blue wash-out, the external beads were still fluorescent (43, 44). Excess dye was removed (two washes with PBS), and phagocytosis was visualized using fluorescence microscopy. On each coverslip, 80 or 180 Raw264.7 cells or transfected IMLFs, respectively, were scored, and ~350 beads per sample were analyzed. Phagocytosis was quantified as the phagocytic index, the number of ingested beads/total number of cells analyzed.

Time-lapse images were obtained using a Zeiss LSM510 inverted confocal microscope system (Carl Zeiss, Gottingen, Germany). Images were acquired at 30-s intervals for a total time of 30 min.

In the second protocol, phagocytosis was assessed by fluorescence-activated cell sorter (FACS) analysis (45, 46). Fluorescence intensity was recorded before (binding) and after 0.1% trypan blue addition (phagocytosis) to quench the fluorescence of the extracellular bound beads. Typically, 2×10^5 events/sample were counted, and the percentages of binding, as the numbers of the fluorescent-positive events (number of cells with beads), were expressed as percentages of total events (number of cells analyzed), and the percentages of phagocytic cells, as the numbers of fluorescent-positive events after trypan blue addition (number of cells with phagocytosed beads), were expressed as percentages of total events.

For the biochemical separation of phagosomes, the procedure was performed as in Ref. 47, with minor modifications. Briefly, phagocytosis was performed as described previously using tosyl-activated M-280 Dynabeads (2.8 μm diameter, Invitrogen). At the indicated times, phagocytosing Raw264.7 cells were scraped into ice-cold lysis buffer (25 mM Tris-HCl, pH 7.4, 0.25 M sucrose, 2.5 mM DTT, 2.5 mM EDTA, 20 mM NaF, 1 mM sodium orthovanadate, 1 mM *p*-nitrophenyl phosphate, 5 mM imidazole, 50 mM *o*-phenanthroline, 2 mM pepstatin, and 1 mM phenylmethylsulfonyl fluoride) and sonicated (two times, 20-s pulses). The beads were isolated on ice using a magnet; the unbound material was removed, and the beads were washed with lysis buffer and then solubilized in Laemmli sample buffer (bead-associated membranes). The unbound material was centrifuged 45 min at 100,000 × *g* at 4 °C; the supernatant (cytosol) was recovered; the pellet was washed with lysis buffer and centrifuged again, and then the final pellet was resuspended in ice-cold lysis buffer and sonicated (one time, 20-s pulse) (non-bead associated membranes). The $PLA_2IV\alpha$ levels in the different fractions were analyzed by Western blotting with the anti-$PLA_2IV\alpha$ rabbit antibody and normalized by the presence of rabbit IgGs (used in the opsonization step) with an HRP-conjugated anti-rabbit antibody (for the bead-associated membranes), by the presence of GM130 with a mouse monoclonal anti-GM130 antibody (Transduction Laboratories, Lexington, KY) for the non-bead associated membranes, and by the presence of GAPDH with a mouse anti-lapine GAPDH antibody (AbD Serotec, Pucheim, Germany).

Phagocytosis of *Listeria monocytogenes* was quantified using a gentamycin-protection assay, as reported previously (48).

Statistical Analysis—All of the data are expressed as means ± S.E. (error bars). Significance was calculated using paired, two-tailed Student's *t* tests, with p values <0.05 considered significant.

RESULTS

FcR-mediated Phagocytosis Selectively Stimulates $PLA_2IV\alpha$—Macrophage responses to *E. coli* lipopolysaccharide (LPS) include the well documented release of arachidonic acid, which is considered to be the link between PLA_2 activity and the inflammatory response (3). Thus, the involvement of PLA_2 in

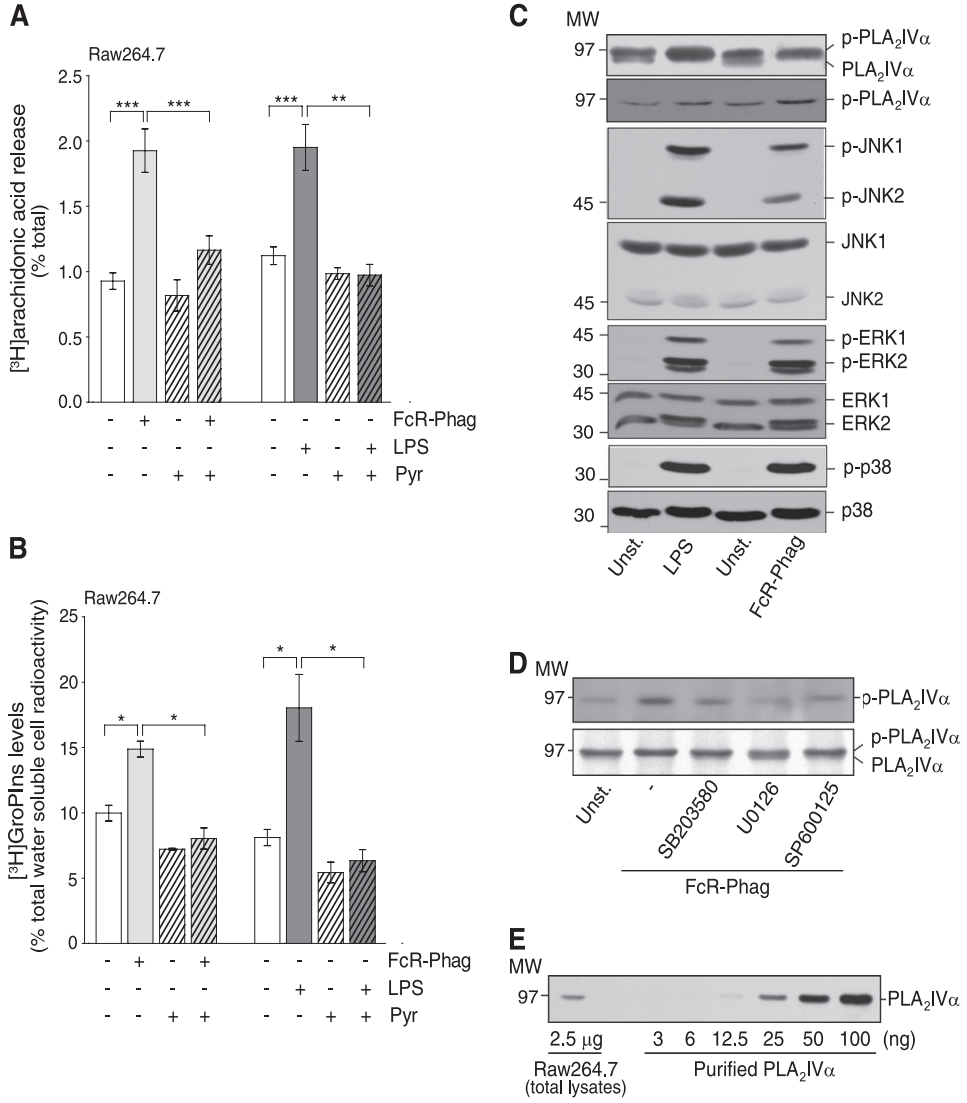

FIGURE 1. **FcR-mediated phagocytosis and LPS activate phosphorylation of PLA$_2$IVα, MAPKs, and stress kinases in Raw264.7 cells.** Cells without (−) or with (+) a 15-min preincubation with 0.5 μM pyrrophenone (*Pyr*) were stimulated by FcR-mediated phagocytosis (*FcR-Phag*) or by 20 μg/ml LPS from *E. coli* for a further 30 and 45 min, respectively, at 37 °C (see "Experimental Procedures"). *A*, [^{3}H]arachidonic acid release (percentage of total [^{3}H]arachidonic acid cell content). Data are means ± S.E. of 10 independent experiments for phagocytosis, each performed in triplicate, and of four independent experiments for LPS stimulation, each performed in duplicate. ***, $p < 0.001$; **, $p < 0.02$ (Student's *t* test). *B*, intracellular [^{3}H]GroPIns production (percentage of total [^{3}H]inositol-labeled water-soluble metabolites). Data are means ± S.E. of at least five independent experiments, each performed in duplicate. *, $p < 0.05$ (Student's *t* test). *C*, representative Western blotting showing PLA$_2$IVα phosphorylation by gel shift or by phosphorylated PLA$_2$IVα, and phosphorylation (*p*-) and total levels of JNK, ERK1/2, and p38 in unstimulated cells (*Unst.*), after 30 min of FcR-mediated phagocytosis or of 20 μg/ml LPS treatments (see "Experimental Procedures"). *D*, representative Western blotting showing phosphorylated PLA$_2$IVα in unstimulated cells (*Unst.*) or after 30 min of FcR-mediated phagocytosis in the absence (−) or presence of 15-min preincubation with 10 μM of the indicated kinase inhibitors. *E*, representative Western blotting of 2.5 μg total Raw264.7 cell lysate and increasing amounts of purified PLA$_2$IVα protein (from 3 to 100 ng, as indicated). *MW*, molecular weight marker (kDa).

FcR-mediated phagocytosis was investigated here in parallel with LPS stimulation in Raw264.7 cells.

PLA$_2$ activity, as assessed by arachidonic acid release, was stimulated to similar extents by FcR-mediated phagocytosis of IgG-opsonized latex beads (3 μm) and treatment with 20 μg/ml LPS, with 1.1- and 0.7-fold increases over basal levels, respectively (Fig. 1*A*). To identify which specific PLA$_2$ is activated, a panel of inhibitors was used that have specificities for the different isoforms of the PLA$_2$ superfamily. Pretreatment of Raw264.7 cells with 0.5 μM pyrrophenone, a selective and reversible inhibitor of the class IV PLA$_2$s (38), nearly completely abolished the effects of both of these stimuli (Fig. 1*A*). In contrast, 50 μM sPLA$_2$IIA inhibitor-I, which inhibits class II and V secretory PLA$_2$s (49), and 1 μM bromoenol lactone, which inhibits group VI PLA$_2$s (50), showed no inhibition of arachidonic acid release stimulated by FcR-mediated phagocytosis (Table 1).

Previous studies from our laboratory characterized PLA$_2$IVα as the specific PLA$_2$ isoform that mediates GroPIns production from the membrane phosphatidylinositol, through the transient formation of lysophosphatidylinositol (lyso-PtdIns) (24). Thus, the selective activation of PLA$_2$IVα by FcR-mediated phagocytosis can be further monitored through the cellular levels of GroPIns, as quantified by HPLC analysis after equilibrium labeling with *myo*-[^{3}H]inositol (see under "Experimental Procedures"). At steady state, GroPIns levels are ~120 μM in

TABLE 1

Modulation of [^{3}H]arachidonic acid release and [^{3}H]GroPIns production induced by FcR-mediated phagocytosis and LPS stimulation in Raw264.7 cells

Raw264.7 cells without or with 15-min preincubations with the different inhibitors, as indicated, were left untreated or were stimulated by FcR-mediated phagocytosis or with 20 μg/ml LPS for a further 30 and 45 min, respectively, at 37 °C (see "Experimental Procedures"). [^{3}H]Arachidonic acid release as percentage of total [^{3}H]arachidonic acid cell content, with basal release before phagocytosis and LPS stimulation of 0.93 ± 0.06 and 1.12 ± 0.07% of total cell content, respectively. Intracellular [^{3}H]GroPIns production as a percentage of total water-soluble [^{3}H]inositol-labeled metabolites, with the basal levels before phagocytosis and LPS stimulation of 9.98% ± 0.60 and 8.12% ± 0.62%, respectively. Data are means ± S.E. of at least four independent experiments, each performed in duplicate. In parallel, under the conditions reported above, lysophosphatidylinositol levels were monitored by TLC (for the method see Ref. 42), with an increase of 0.3- and 0.8-fold over basal for stimulation by FcR-mediated phagocytosis and LPS, respectively, effects that were completely blocked by pyrrophenone treatment. ND means not determined.

	[^{3}H]arachidonic acid release (% total cell content)			[^{3}H]GroPIns production (% total water-soluble [^{3}H]inositol cell content)		
Condition (target)	Unstimulated	FcR-phagocytosis	LPS	Unstimulated	FcR-phagocytosis	LPS
Control		1.93 ± 0.17[a]	1.95 ± 0.18[a]		14.88 ± 0.61[b]	18.03 ± 2.56[b]
0.5 μM Pyr (PLA$_2$IVα)	0.98 ± 0.04	0.97 ± 0.08[c]	0.97 ± 0.08[a]	5.44 ± 0.79	8.04 ± 0.81[b]	6.34 ± 0.85[b]
1 μM BEL (PLA$_2$VI)	1.03 ± 0.06	2.00 ± 0.08	1.55 ± 0.10	6.42 ± 0.41	16.33 ± 0.01	19.91 ± 0.81
50 μM sPLA$_2$IIA inhibitor-I (sPLA$_2$)	1.16 ± 0.07	2.10 ± 0.04	1.69 ± 0.27	10.31 ± 1.05	21.14 ± 0.01	20.54 ± 2.76
10 μM SB203580 (p38)	1.30 ± 0.11	1.35 ± 0.06[c]	1.83 ± 0.32	6.08 ± 0.62	ND	13.49 ± 2.56
10 μM U0126 (ERK1/2)	1.16 ± 0.28	1.25 ± 0.04[c]	1.08 ± 0.17[b]	5.81 ± 0.62	ND	6.39 ± 0.62[b]
10 μM SP600125 (JNK)	1.16 ± 0.04	1.20 ± 0.03[a]	2.61 ± 0.04	ND	ND	ND
10 μM SB203580 + 10 μM U0126 (p38 + ERK1/2)	ND	0.87 ± 0.15[c]	ND	ND	ND	ND

[a] $p < 0.001$ (Student's t test), with respect to their relevant controls.
[b] $p < 0.05$ (Student's t test), with respect to their relevant controls.
[c] $p < 0.02$ (Student's t test), with respect to their relevant controls.

Raw264.7 cells, as assessed using mass spectrometry (for methods, see Refs. 42, 51). Indeed, here the FcR-mediated phagocytosis and LPS stimulation specified above also increased the intracellular levels of GroPIns (0.5- and 1.2-fold over basal, respectively; Fig. 1*B*). This GroPIns production was PLA$_2$IVα-dependent, as it was completely inhibited by treatment with 0.5 μM pyrrophenone (Fig. 1*B*); in contrast, the inhibitors of secretory PLA$_2$s and group VI PLA$_2$s did not inhibit this GroPIns production (Table 1).

As PLA$_2$IVα phosphorylation has been associated with its activation (52), the levels of phosphorylated PLA$_2$IVα were followed by Western blotting of Raw264.7 cell lysates. As shown in Fig. 1*C*, phosphorylated PLA$_2$IVα can be distinguished from its nonphosphorylated form as it runs as a distinct upper band (24). Moreover, an anti-phospho-PLA$_2$IVα antibody was used to specifically monitor phosphorylation of PLA$_2$IVα on Ser-505. These approaches showed that under basal conditions, the level of phosphorylated PLA$_2$IVα was higher than the nonphosphorylated form, and upon FcR-mediated phagocytosis and LPS stimulation, PLA$_2$IVα was completely shifted to the higher molecular weight, and there was a corresponding ~70% increase in Ser-505 phosphorylation (Fig. 1*C*). Among the kinases known to regulate PLA$_2$IVα, both the MAPKs ERK1/2 and the stress kinases p38 and JNK were phosphorylated by FcR-mediated phagocytosis and LPS stimulation and consequently activated (Fig. 1*C*). In addition, inhibitors specific for these three kinases (U0126 for ERK1/2; SB203580 for p38; and SP600125 for JNK; all at 10 μM) reduced the phagocytosis-induced PLA$_2$IVα phosphorylation (Fig. 1*D*) and blocked the phagocytosis-induced arachidonic acid release (>90% inhibition) (Table 1), which indicates that these MAPKs and stress kinases are upstream of PLA$_2$IVα activity.

These analyses of arachidonic acid and GroPIns production demonstrate that during FcR-mediated phagocytosis in Raw264.7 cells PLA$_2$IVα is selectively activated and regulated by multiple kinases. In addition, quantification of PLA$_2$IVα protein levels demonstrated that PLA$_2$IVα is an abundant protein in these cells, with ~7 ng/μg total cell lysate protein (Fig. 1*E*).

PLA$_2$IVα Participates in FcR-mediated Phagocytosis—To determine the role of PLA$_2$IVα in the uptake of IgG-opsonized particles, we first analyzed this in Raw264.7 professional phagocytic cells and then in fibroblasts modified for phagocytosis. This was carried out by immunofluorescence, using fluorescence microscopy for morphological analyses and FACS for automated quantification. These two analytical procedures produced similar results.

Pretreatment of the Raw264.7 cells with 0.5 μM pyrrophenone induced a 50% reduction in opsonized particle uptake, which was seen as a reduced phagocytic index and percent of phagocytosis (Fig. 2*A* and Table 2), with no interference in particle binding to the cells (Table 2). This inhibition by pyrrophenone was, however, not as large as that of 10 μM cytochalasin D, a potent inhibitor of actin polymerization, and consequently of phagocytosis (Fig. 2*A* and Table 2), but it was retained during the overall time course of the phagocytosis analysis (from 0 to 120 min). In contrast, treatments with bromoenol lactone and sPLA$_2$IIA inhibitor-I were ineffective (Table 2). In parallel with this pharmacological approach, we also attempted to silence PLA$_2$IVα expression using both small interfering siRNAs and vectors coding for short hairpin shRNAs; however, in both of these cases, the reduction in PLA$_2$IVα protein levels reached was never sufficient to perform biochemical assays (data not shown).

To confirm the phagocytosis inhibition obtained with pyrrophenone in Raw264.7 cells, an alternative model was chosen based on SV40 IMLFs from wild-type (IMLF$^{+/+}$ cells) and PLA$_2$IVα knock-out (IMLF$^{-/-}$ cells) mice (39). As with all fibroblasts, these are autophagocytosing cells, and transfection of the Fcγ receptor IIA (FcγR) is sufficient to promote phagocytosis of IgG-opsonized particles (53, 54).

First, we verified the endogenous expression levels of PLA$_2$IVα in the IMLF$^{+/+}$ cells by Western blotting, along with the equal overexpression levels of the FcγR both without and

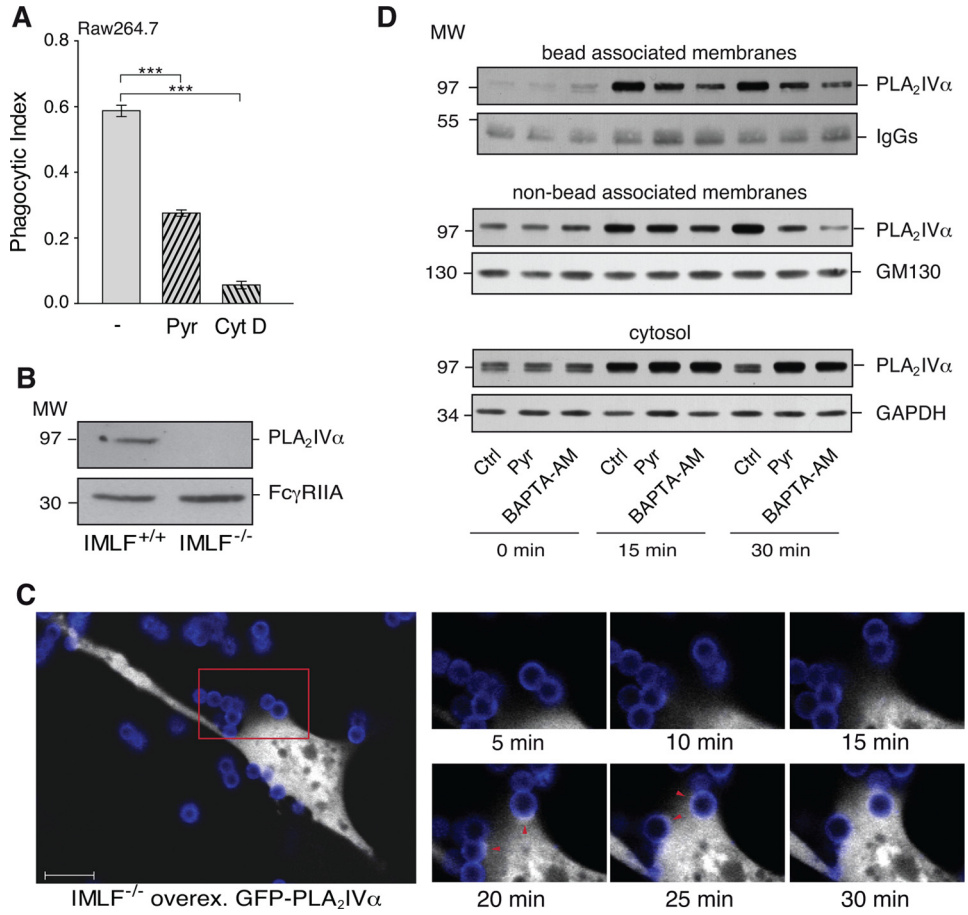

FIGURE 2. **PLA$_2$IVα is a component of the phagocytic machinery formed consequent to FcR activation.** Raw264.7 cells were stimulated by FcR-mediated phagocytosis of IgG-opsonized latex beads for 30 min at 37 °C, and particle uptake/binding was quantified. *A*, quantification of phagocytosed beads by fluorescence microscopy. Phagocytosis was performed in the absence (−) and presence of a 15-min pretreatment with 0.5 μM pyrrophenone (*Pyr*) or 10 μM cytochalasin D (*Cyt D*). Data are expressed as phagocytic index and represent means ± S.E. of eight independent experiments. ***, $p < 0.001$ (Student's t test). *B*, representative Western blotting showing expression of endogenous PLA$_2$IVα (*top*) and overexpressed FcγR (*bottom*) in IMLF$^{+/+}$ and IMLF$^{-/-}$ cells. *C*, time-lapse microscopy images showing PLA$_2$IVα localization during FcR-mediated phagocytosis. IMLF$^{-/-}$ cells were grown in live cell imaging dishes and transfected with FcγR and GFP-PLA$_2$IVα and then used in the phagocytosis assay in a thermostated chamber under the microscope. FcγR-mediated phagocytosis was followed under fluorescence microscopy. The large panel (*left*) shows a single IMLF$^{-/-}$ cell transfected with GFP-PLA$_2$IVα (*white*) in the presence of Alexa546-labeled IgG-opsonized beads (*blue*). *Scale bar*, 10 μm. The smaller panels (*right*) are higher magnifications of the *red square* outlined in the larger panel, as frames were collected at the times indicated. The *arrowheads* (20–25 min) indicate GFP-PLA$_2$IVα localization at the phagocytic cup. *D*, localization of endogenous PLA$_2$IVα during FcR-mediated phagocytosis in Raw264.7 cells. Phagocytosis was performed in the absence (*Ctrl*) and presence of a 15-min pretreatment with 0.5 μM pyrrophenone (*Pyr*) or a 5-min pretreatment with 10 μM BAPTA-AM (incubated in the last minutes of opsonized bead binding). At the indicated times (0, 15, and 30 min), phagocytosis was terminated, and the nascent phagosomes (bead-associated membranes), total cell membranes (non-bead-associated membranes), and cytosolic fractions (*cytosol*) were recovered and subjected to Western blotting (see "Experimental Procedures"). Data are representative of three independent experiments.

with the PLA$_2$IVα knock-out (Fig. 2*B*). Equal FcγR expression was also confirmed by the similar levels of binding of IgG-opsonized beads with these IMLF$^{+/+}$ and IMLF$^{-/-}$ cell lines (Table 2). In the IMLF$^{-/-}$ cells, FcγR-mediated phagocytosis was 50% of that seen for the IMLF$^{+/+}$ cells and was insensitive to treatment with 0.5 μM pyrrophenone (Table 2). Instead, in the IMLF$^{+/+}$ cells, 0.5 μM pyrrophenone reduced the FcγR-mediated phagocytosis by 50%, thus corresponding to the baseline phagocytosis of the IMLF$^{-/-}$ cells (Table 2). This inhibition of phagocytosis was similar to that seen in the Raw264.7 cells (Fig. 2*A* and Table 2). In addition, transfection of PLA$_2$IVα in IMLF$^{-/-}$ cells promoted increased phagocytosis, which indeed reached levels comparable with the wild-type IMLF$^{+/+}$ cells (Table 2).

With these IMLF$^{-/-}$ cells co-transfected with FcγR and GFP-PLA$_2$IVα, we also took advantage of the possibility to monitor the PLA$_2$IVα cellular localization during FcγR-mediated phagocytosis using confocal microscopy. Here, time-lapse video microscopy revealed that GFP-PLA$_2$IVα was initially diffuse in the cytosol. After the promotion of phagocytosis through binding of the opsonized particles to the FcγR in IMLF$^{-/-}$ cells, the GFP-PLA$_2$IVα translocated to the nascent phagosomes at the level of the phagocytic cup; it then completely surrounded the particles as they were endocytosed. At the end of the process, GFP-PLA$_2$IVα was again diffuse in the cytosol (Fig. 2*C* and supplemental Movies S1.A and S1.B). In the control IMLF$^{-/-}$ cells transfected for GFP alone, this GFP remained diffuse in the cytosol, without changing its localization, during the entire process of phagocytosis (supplemental Movie S2). Similar *in vivo* video microscopy studies in Raw264.7 cells could not be performed due to the abundant endogenous PLA$_2$IVα, which interferes with the correct localization of overexpressed GFP-PLA$_2$IVα. Instead, in these Raw264.7 cells the association of endogenous PLA$_2$IVα

TABLE 2

Modulation of FcR-mediated phagocytosis

Cells without or with a 15-min preincubation with different inhibitors, as indicated, were incubated in the absence or presence of IgG-opsonized latex beads for 30 min at 37 °C, and both particle binding (FcR binding, before trypan blue addition) and uptake (FcR phagocytosis, after trypan blue addition) were quantified by FACS analysis. For BAPTA-AM, the addition started in the last 5 min of opsonized bead binding. FcR-mediated phagocytosis of untreated Raw264.7 cells (time 0) was 0.65 ± 0.4%. IMLF cells were from PLA$_2$IVα wild-type (IMLF$^{+/+}$) and PLA$_2$IVα knock-out (IMLF$^{-/-}$) mice, and they were transfected with FcγR and the different constructs, as indicated in the left-hand column. When GFP-tagged constructs were expressed, only transfected cells were analyzed, instead of the total population (see under "Experimental Procedures"). Data are expressed as percentages of total analyzed cells and represent means ± S.E. of at least four independent experiments.

Cell type	Condition (target)	FcR-binding (% binding)	FcR-phagocytosis (% phagocytosis)
Raw264.7 cells	Control	27.1 ± 4.3	25.2 ± 4.6
	Cyt D	29.7 ± 2.0	1.2 ± 0.2[a]
	0.5 μM Pyr (PLA$_2$IVα)	30.3 ± 2.2	12.2 ± 1.1[c]
	1 μM BEL (PLA$_2$VI)	29.2 ± 5.8	26.1 ± 5.8
	50 μM sPLA$_2$IIA inhibitor-I (sPLA$_2$)	32.9 ± 6.2	31.0 ± 5.3
	10 μM BAPTA-AM (calcium)	24.9 ± 1.9	12.2 ± 0.8
	10 μM SB203580 (p38)	22.8 ± 3.3	21.0 ± 4.3
	10 μM U0126 (ERK1/2)	23.1 ± 4.0	21.9 ± 5.8
	10 μM SB203580 + 10 μM U0126 (p38 + ERK1/2)	22.5 ± 4.9	20.7 ± 5.8
IMLF$^{+/+}$	Control	3.6 ± 0.8	1.7 ± 0.4
	0.5 μM Pyr (PLA$_2$IVα)	3.3 ± 1.2	0.9 ± 0.3[a]
IMLF$^{-/-}$	Control	3.6 ± 0.7	0.9 ± 0.1[b]
	0.5 μM Pyr (PLA$_2$IVα)	3.4 ± 1.3	0.9 ± 0.3
IMLF$^{-/-}$ over-expression PLA$_2$IVα	Control	3.1 ± 1.6	1.6 ± 0.1[a]
IMLF$^{-/-}$ over-expression GFP	Control	10.5 ± 1.0	2.0 ± 1.0
IMLF$^{-/-}$ over-expression GFP-PLA$_2$IVα	Control	16.1 ± 1.8	12.1 ± 1.0
	0.5 μM Pyr (PLA$_2$IVα)	14.9 ± 1.2	6.7 ± 0.6[a]
IMLF$^{-/-}$ over-expression GFP-PLA$_2$IVα(1-525)	Control	12.8 ± 1.0	13.2 ± 2.0
	0.5 μM Pyr (PLA$_2$IVα)	15.0 ± 1.0	16.7 ± 1.5
IMLF$^{-/-}$ over-expression GFP-PLA$_2$IVα-S228C	Control	19.3 ± 5.1	13.9 ± 2.0
	0.5 μM Pyr (PLA$_2$IVα)	15.5 ± 5.8	6.1 ± 2.6[a]
IMLF$^{-/-}$ over-expression GFP-C2-dom.	Control	13.9 ± 1.0	12.0 ± 1.0
	0.5 μM Pyr (PLA$_2$IVα)	14.2 ± 1.0	12.2 ± 1.0
IMLF$^{-/-}$ over-expression GFP-PLA$_2$IVα-D43N	Control	18.3 ± 3.5	1.8 ± 0.9

[a], $p < 0.05$; [b], $p < 0.02$; [c], $p < 0.001$ (Student's *t*-test), with respect to their relevant controls.

with the phagosomal membranes was directly evaluated using a biochemical approach. During synchronized phagocytosis, PLA$_2$IVα was enriched in the membrane fractions in a time-dependent manner (from 1 to 20 min), with a parallel decrease of its levels in the cytosolic fraction (not shown).

Because Ca^{2+} is considered the main regulator of PLA$_2$IVα membrane translocation (11), the effects on PLA$_2$IVα localization of an intracellular Ca^{2+} chelator (10 μM BAPTA-AM) and also of pyrrophenone were monitored. By Western blotting, both PLA$_2$IVα phagosome translocation (bead associated membranes in Fig. 2*D*) and total membrane translocation (non-bead associated membranes, Fig. 2*D*) were analyzed in phagocytosing Raw264.7 cells. Treatment with BAPTA-AM and pyrrophenone inhibited PLA$_2$IVα membrane translocation by ~80 and 50%, respectively (Fig. 2*D*). A similar inhibition by BAPTA-AM and pyrrophenone on PLA$_2$IVα membrane association was confirmed also by confocal microscopy in IMLF$^{-/-}$ cells expressing GFP-PLA$_2$IVα, and whenever a phagosome was present in cells treated with both agents, no enrichment of PLA$_2$IVα was observed at the phagosomal level (Movies S3A–C). The effects of BAPTA-AM on PLA$_2$IVα membrane translocation was seen as 50% inhibition of FcR-induced phagocytosis without any significant effects on bead binding (Table 2).

Altogether, these data indicate that PLA$_2$IVα is a component of the phagocytic machinery that is formed consequent to FcR activation, thus regulating opsonized particle uptake. However, pyrrophenone inhibition of both PLA$_2$IVα enzymatic activity and membrane translocation questioned the possible mechanism of action of PLA$_2$IVα in the regulation of the phagocytosis process.

PLA$_2$IVα Regulates FcR-mediated Phagocytosis via a Nonenzymatic Mechanism—A number of studies have suggested an involvement of PLA$_2$s in the process of phagocytosis, through the actions of PLA$_2$ metabolites on membrane curvature (19, 32). Indeed, PLA$_2$ hydrolysis of the outer leaflet of the membrane bilayer can result in the conversion of cylindrical and cone-shaped phospholipids into inverted cone-shaped lysophospholipids, which can stimulate or initiate membrane bending (16).

The requirement for the enzymatic activity of PLA$_2$IVα in FcR-mediated phagocytosis was directly assessed using the co-expression of FcγR and GFP-tagged PLA$_2$IVα wild-type or mutated versions (Fig. 3*A*) in the IMLF$^{-/-}$ cells, with the GFP allowing the monitoring of the transfected cells. As verified by Western blotting, under these conditions the overexpression levels of GFP-PLA$_2$IVα were always lower than the endogenous levels in Raw264.7 cells (Fig. 3*B* and its legend). Unexpectedly, overexpression of the GFP-PLA$_2$IVα(1–525) deletion mutant of PLA$_2$IVα (without a complete catalytic domain, and therefore without enzymatic activity; Fig. 3, *A* and *C*, and Ref. 36) rescued the impaired phagocytosis of these IMLF$^{-/-}$ cells (Fig. 3*D* and Table 2).

To investigate whether the membrane binding of PLA$_2$IVα is sufficient to regulate FcγR-mediated phagocytosis even in the absence of PLA$_2$IVα catalytic activity, another catalytically inactive PLA$_2$IVα mutant was used: GFP-PLA$_2$IVα-S228C, with a single point mutation in the catalytic domain (55), and the GFP-PLA$_2$IVα-C2 domain, because membrane localization of PLA$_2$IVα is mainly driven by the insertion of its N-terminal C2 domain into the lipid bilayer (Fig. 3*A*) (11). When this GFP-PLA$_2$IVα-S228C mutant or the PLA$_2$IVα-C2 domain was co-transfected with FcγR in the IMLF$^{-/-}$ cells, phagocytosis increased to a level comparable with transfection of the wild-type GFP-PLA$_2$IVα (Fig. 3, *C* and *D*, and Table 2).

To further confirm the necessity for PLA$_2$IVα membrane binding for rescue of this impaired FcγR-mediated phagocytosis, another PLA$_2$IVα point mutant was used, *i.e.* GFP-PLA$_2$IVα-D43N, with a single point mutation in the C2 domain that prevents its membrane translocation (Fig. 3, *A* and *C*) (12). GFP-PLA$_2$IVα-D43N co-expression with FcγR in these IMLF$^{-/-}$ cells induced a small increase in the basal phagocytosis index that was not comparable with that of the wild-type PLA$_2$IVα protein (Fig. 3*D*). This might be a consequence of the high overexpression levels of this GFP-PLA$_2$IVα-D43N mutant, which would lead to its partial membrane mislocalization. None of these constructs significantly affected the binding of the opsonized particles to the IMLF$^{-/-}$ cells (Table 2).

Under these conditions, we also monitored the effects of pyrrophenone treatment on the rescue of FcR-mediated phagocy-

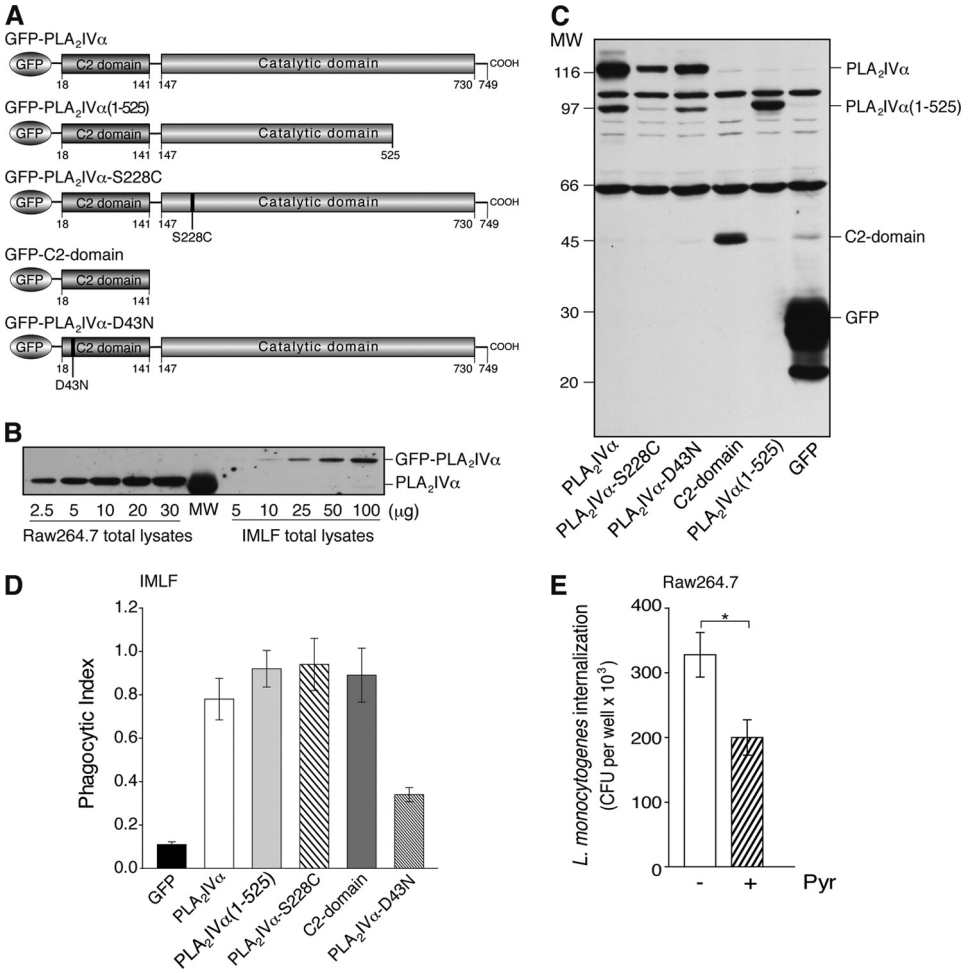

FIGURE 3. **PLA$_2$IVα enzymatic activity is not necessary for productive FcR-mediated phagocytosis.** *A*, schematic representation of GFP-PLA$_2$IVα and PLA$_2$IVα deletion and point mutants. GFP-PLA$_2$IVα is characterized by an N-terminal C2 domain and a C-terminal catalytic domain. The GFP-PLA$_2$IVα-C2-domain, the deleted mutant GFP-PLA$_2$IVα(1–525), and the point mutant GFP-PLA$_2$IVα-S228C have no catalytic activity, but they translocate to membranes under agonist stimulation (18, 36, 55). The point mutant GFP-PLA$_2$IVα-D43N cannot translocate to membranes under cell stimulation (12). *B*, representative Western blotting of 2.5–30 and 5–100 μg total lysates from Raw264.7 and IMLF$^{-/-}$ cells overexpressing GFP-PLA$_2$IVα, respectively. IMLF$^{-/-}$ transfection efficiency was 30%, as verified by FACS analysis, independent of transfection construct, and the estimated total protein was ~520 and ~350 pg/cell for Raw264.7 and IMLF$^{-/-}$ cells, respectively. The PLA$_2$IVα protein content was comparable between 3 μg of Raw264.7 cell lysate and 100 μg of IMLF$^{-/-}$ cell lysate. Thus, assuming uniform overexpression of GFP-PLA$_2$IVα and taking into account the efficiency of transfection, the protein levels reached in PLA$_2$IVα-transfected IMLF$^{-/-}$ cells was one-tenth that of the endogenous level in Raw264.7 cells. *C*, representative Western blotting of transfection levels of GFP and GFP-PLA$_2$IVα (wild-type and mutants, as indicated) in IMLF$^{-/-}$ cells, followed using an anti-GFP antibody (see "Experimental Procedures"). Data are representative of at least four independent experiments. *D*, quantification by morphological analysis of particle uptake (phagocytic index) in IMLF$^{-/-}$ cells transfected with FcγR ± GFP or with different GFP-PLA$_2$ constructs (as indicated). Data represent means ± S.E. of at least four independent quantifications. *E*, internalization of *L. monocytogenes* in Raw264.7 cells. Cells were infected with bacteria (multiplicity of infection of 10) for 1 h at 37 °C, and internalization was quantified using the gentamicin protection assay (see "Experimental Procedures") in the absence (−) and presence (+) of 0.5 μM pyrrophenone (30-min pretreatment), and expressed as colony forming units per well. In control proliferation assays, pyrrophenone did not affect *L. monocytogenes* growth (up to 10 h of pyrrophenone treatment). Data are means ± S.D. of nine independent experiments, each performed in triplicate. *, $p < 0.05$ (Student's *t* test).

tosis by the different PLA$_2$IVα mutants in IMLF$^{-/-}$ cells. Here, pyrrophenone impaired the recovery of phagocytosis consequent to overexpression of GFP-PLA$_2$IVα-S228C (~50% inhibition) (Table 2). Instead, pyrrophenone was inactive when the PLA$_2$IVα(1–525) deletion mutant or the PLA$_2$IVα C2 domain was expressed in the same system (Table 2). Of note, neither of these two proteins contain a complete catalytic domain and hence the PLA$_2$IVα-binding site for pyrrophenone (56).

Indeed, time-lapse video microscopy studies in transfected IMLF$^{-/-}$ cells showed that GFP-PLA$_2$IVα-S228C, PLA$_2$IVα(1–525), and PLA$_2$IVα C2 domain all translocate to the phagosomal membranes during FcR-mediated phagocytosis, but pyrrophenone treatment can only impair the membrane association of PLA$_2$IVα-S228C (supplemental Movies S4.A and B, S5.A and B, and S6.A and B). This suggests that the catalytically inactive mutant PLA$_2$IVα-S228C can still bind pyrrophenone, which inhibits PLA$_2$IVα-S228C membrane translocation and impairs PLA$_2$IVα-S228C rescue of phagocytosis in IMLF$^{-/-}$ cells, similar to wild-type PLA$_2$IVα.

As an alternative to pyrrophenone, a combination of the inhibitors of the two main upstream kinases of PLA$_2$IVα activation was used in the Raw264.7 cells (U0126 and SB203580; both at 10 μM). Here, both phagocytosis-induced release of arachidonic acid and FcR-mediated phagocytosis were monitored. The PLA$_2$IVα enzymatic activity was completely inhibited by this treatment (Table 1), whereas FcR-mediated phago-

TABLE 3

Modulation of FcR-mediated phagocytosis by PLA$_2$ metabolites and arachidonate pathway inhibitors

Raw264.7 cells without or with a 15-min preincubation with different compounds, as indicated, were incubated in the presence of IgG-opsonized latex beads for 30 min at 37 °C, and both the particle binding (FcR binding; before trypan blue addition) and uptake (FcR phagocytosis; after trypan blue addition) were quantified by FACS analysis. Data are means ± S.E. of at least four independent experiments. 5-LOX, 5-lipoxygenase; PGE, prostaglandin E; TxB$_2$, thromboxane B$_2$; LT, leukotrienes.

Condition	FcR binding (% binding)	FcR phagocytosis (% phagocytosis)
Control	27.1 ± 1.1	20.1 ± 0.5
10 μM (30 μM) lyso-PtdIns	25.3 ± 1.5 (25.3 ± 2.1)	19.1 ± 0.8 (18.8 ± 1.1)
300 μM GroPIns	25.5 ± 2.5	16.6 ± 1.1
50 μM GroPIns4*P*	26.8 ± 1.7	14.8 ± 0.4[a]
50 μM GroPIns4,5P_2	25.9 ± 1.2	13.5 ± 0.3[a]
0.1 μM (1 μM) arachidonic acid	30.4 ± 1.0 (27.9 ± 0.6)	23.6 ± 1.0 (20.2 ± 0.8)
300 μM lysine salt of acetylsalicylic acid (COX1/2 inhibitor)	27.5 ± 1.5	19.0 ± 1.9
10 μM ketoconazole (thromboxane synthase and 5-LOX inhibitor)	29.0 ± 1.7	21.5 ± 1.4
5 μM LY83583 (leukotriene synthesis inhibitor)	29.1 ± 3.8	23.9 ± 2.4
10 μM NS5398 (COX2 inhibitor)	29.5 ± 2.4	21.0 ± 4.1
10 μM REV5901 (antagonist of LTD$_4$ receptors)	28.5 ± 3.1	21.2 ± 1.1
100 nM PGE$_1$	27.6 ± 2.1	21.9 ± 1.7
100 nM PGE$_2$	29.6 ± 2.5	20.2 ± 2.0
100 nM TxB$_2$	25.7 ± 1.0	17.9 ± 1.0
100 nM LTB$_4$	28.4 ± 1.2	21.0 ± 1.7
100 nM LTC$_4$	28.4 ± 0.6	19.6 ± 0.6
100 nM LTD$_4$	27.1 ± 3.1	21.0 ± 2.0
100 nM LTE$_4$	27.9 ± 4.3	21.1 ± 3.2

[a] $p < 0.02$ (Student's *t*-test), with respect to their relevant controls.

cytosis was not significantly affected (Table 2). This further demonstrates that PLA$_2$IVα modulates the phagocytic process independent of its enzymatic activity also in an endogenous expression system and thus under physiologically relevant conditions.

PLA$_2$IVα Metabolites Do Not Regulate FcR-mediated Phagocytosis—To further exclude a role for the PLA$_2$IVα catalytic activity in FcR-mediated phagocytosis, some of the PLA$_2$IVα metabolites that were detected in Raw264.7 cells during phagocytosis were tested and excluded for their involvement in this process (Table 3). As shown under "FcR-mediated Phagocytosis Selectively Stimulates PLA$_2$IVα," in Raw264.7 cells FcR-mediated phagocytosis can induce the production of GroPIns and its precursor lyso-PtdIns (Table 1 and its legend), which might be a mediator of PLA$_2$IVα activity on membrane curvature. To define the role of these metabolites in the regulation of the phagocytic process, lyso-PtdIns (10–30 μM) and for completeness also GroPIns, GroPIns4*P*, and GroPIns4,5P_2 (300, 50, and 50 μM, respectively) were added exogenously to Raw264.7 cells, and the uptake of IgG-opsonized beads was monitored. As shown in Table 3, this uptake was insensitive to these lyso-PtdIns and GroPIns treatments; in contrast, it was inhibited by 25 and 30% by GroPIns4*P* and GroPIns4,5P_2, respectively.

In addition, the alternative downstream pathways activated by PLA$_2$IVα that mainly involves arachidonic acid metabolism were analyzed. Blockers of the arachidonate pathway and arachidonic acid derivatives were added to phagocytosing Raw264.7 cells, and they did not significantly affect the uptake of opsonized-particles (Table 3). Altogether, these data demonstrate that it is not the enzymatic activity, but it is the membrane binding of PLA$_2$IVα that is required for the regulation of FcR-mediated phagocytosis.

PLA$_2$IVα Involvement in Phagocytosis of Zymosan and Bacteria—In addition to the data shown for the opsonized latex beads, this study of the role of PLA$_2$IVα was extended to different types of phagocytosis, including the uptake of zymosan particles (derived from the *S. cerevisiae* cell wall) and of *L. monocytogenes*. The uptake of zymosan particles was measured by FACS analysis, and the results show that 0.5 μM pyrrophenone had little inhibitory effect on the internalization of zymosan particles in Raw264.7 cells (~15% reduction). This indicates that PLA$_2$IVα has only a marginal role in the pathway triggered by zymosan particle binding to the β-glucan receptor and in its consequent internalization in Raw264.7 cells. *L. monocytogenes* internalization was measured by incubating Raw264.7 cells with the living bacteria, and treatment with 0.5 μM pyrrophenone induced a reduction in *L. monocytogenes* phagocytosis by 40% (Fig. 3*E*). Thus, we can conclude here that PLA$_2$IVα is specifically required during FcR-mediated phagocytosis and for internalization of bacteria, such as *L. monocytogenes*.

DISCUSSION

This study shows the selective phosphorylation, activation, and translocation of PLA$_2$IVα to the membrane of nascent phagosomes during FcR-mediated phagocytosis. Moreover, PLA$_2$IVα is shown not only to be part of the FcR-mediated phagocytosis signaling machinery, but also to actively modulate the uptake of IgG-opsonized particles. This was achieved using two alternative approaches, a potent and selective PLA$_2$IVα inhibitor (pyrrophenone) and cells from PLA$_2$IVα knock-out mice (IMLF$^{-/-}$ cells). Indeed, under both of these conditions, although not completely blocked, FcR-mediated phagocytosis was reduced by 50%. The residual phagocytic activity that is maintained in the absence of PLA$_2$IVα appears to be due to alternative regulatory pathways, producing a redundancy of the phagocytic processes. As phagocytosis is a central process for the survival of any organism, it can be expected that such an essential process also has "fail-safe" mechanisms (30).

An intriguing part of this study is the demonstration that PLA$_2$IVα regulates FcR-mediated phagocytosis independent of its enzymatic activity, which highlights a new mechanism of action for PLA$_2$IVα. Thus, the inhibition of FcR-mediated phagocytosis observed using pyrrophenone in Raw264.7 cells is not simply due to inhibition of PLA$_2$IVα catalytic activity. Here, we demonstrate that the interaction between pyrrophenone and PLA$_2$IVα generates an allosteric block, with the consequent inhibition of membrane translocation of PLA$_2$IVα and the consequent impairment of FcR-mediated phagocytosis. Moreover, the main products of PLA$_2$IVα enzymatic activity (arachidonic acid, arachidonate pathway derivatives, lyso-PtdIns, and the glycerophosphoinositols) do not contribute in any positive ways to the modulation of FcR-mediated phagocytosis.

Through these data, we have thus built a model in which the binding of PLA$_2$IVα to the plasma membrane lipid bilayer appears sufficient to regulate phagosome formation. In addition, in the IMLF$^{-/-}$ cells from the PLA$_2$IVα knock-out mice, the PLA$_2$IVα N-terminal C2 domain was identified as the portion of PLA$_2$IVα that is sufficient to induce a rescue of impaired FcR-mediated phagocytosis. This is in agreement with previous studies, also from our laboratory, that have indicated the C2 domain as the minimal PLA$_2$IVα portion that can still translocate to cell membranes following increases in intracellular Ca^{2+} (18).

Based on the data presented here, we speculate on a new mechanism of action of PLA$_2$IVα, whereby membrane insertion of the PLA$_2$IVα C2 domain induces perturbation of the membrane phospholipid packing, potentially also generating the membrane bending that is necessary for phagosome formation (57). This mechanism of membrane bending has been typically described for proteins that have lipid-binding domains, and a reference model can be seen with synaptotagmin I (58). Comparative analyses between the C2 domains of PLA$_2$IVα and synaptotagmin I also show strong similarities, both in terms of their sequences and their tertiary structures, which would indeed be in favor of a similar mechanism of action for PLA$_2$IVα (59).

The model proposed in this study, which sees a lack of involvement of PLA$_2$IVα enzymatic activity in FcR-mediated phagocytosis, is supported by data obtained with heterologous expression systems that take advantage of the PLA$_2$IVα knock-out mouse model and also with the professional phagocytosing cell line Raw264.7 cells. The molecular mechanisms through which membrane translocation of the PLA$_2$IVα C2 domain is sufficient to promote phagocytic cup formation remain to be defined and will be part of further studies.

Because PLA$_2$IVα metabolite production was monitored during phagocytosis, we propose that PLA$_2$IVα enzymatic activity is not relevant for the phagocytosis process *per se* but is required for bacterial killing (through NADPH oxidase activation and the consequent peroxide production) and for proinflammatory responses (through the production of lipid mediators, such as the eicosanoids and platelet-activating factor).

Acknowledgments—We thank all who kindly provided constructs and reagents (as listed under "Experimental Procedures"); M. A. De Matteis, A. Luini, R. S. Polishchuk, and C. Puri for critical reading of the manuscript; C. P. Berrie for critical reading of and editorial assistance with the manuscript; G. Di Tullio and M. Santoro for preparation of the anti-PLA$_2$IVα antibody; L. Dragani (Consorzio Mario Negri Sud) for the mass spectrometry measurement of GroPIns; the FACS Facility at the Consorzio Mario Negri Sud and the Joint FACS Facility of the Institute of Genetics and Biophysics and Institute of Protein Biochemistry, Naples, Italy, for support in data processing and analysis.

REFERENCES

1. Burke, J. E., and Dennis, E. A. (2009) Phospholipase A$_2$ biochemistry. *Cardiovasc. Drugs Ther.* **23,** 49–59
2. Pérez-Chacón, G., Astudillo, A. M., Balgoma, D., Balboa, M. A., and Balsinde, J. (2009) Control of free arachidonic acid levels by phospholipases A$_2$ and lysophospholipid acyltransferases. *Biochim. Biophys. Acta* **1791,** 1103–1113
3. Funk, C. D. (2001) Prostaglandins and leukotrienes. Advances in eicosanoid biology. *Science* **294,** 1871–1875
4. Shimizu, T. (2009) Lipid mediators in health and disease. Enzymes and receptors as therapeutic targets for the regulation of immunity and inflammation. *Annu. Rev. Pharmacol. Toxicol.* **49,** 123–150
5. Boyanovsky, B. B., and Webb, N. R. (2009) Biology of secretory phospholipase A$_2$. *Cardiovasc. Drugs Ther.* **23,** 61–72
6. Balsinde, J., Bianco, I. D., Ackermann, E. J., Conde-Frieboes, K., and Dennis, E. A. (1995) Inhibition of calcium-independent phospholipase A$_2$ prevents arachidonic acid incorporation and phospholipid remodeling in P388D1 macrophages. *Proc. Natl. Acad. Sci. U.S.A.* **92,** 8527–8531
7. Ohto, T., Uozumi, N., Hirabayashi, T., and Shimizu, T. (2005) Identification of novel cytosolic phospholipase A$_2$s, murine cPLA$_2$δ, -ϵ, and -ζ, which form a gene cluster with cPLA$_2$β. *J. Biol. Chem.* **280,** 24576–24583
8. Bonventre, J. V., Huang, Z., Taheri, M. R., O'Leary, E., Li, E., Moskowitz, M. A., and Sapirstein, A. (1997) Reduced fertility and postischemic brain injury in mice deficient in cytosolic phospholipase A$_2$. *Nature* **390,** 622–625
9. Uozumi, N., Kume, K., Nagase, T., Nakatani, N., Ishii, S., Tashiro, F., Komagata, Y., Maki, K., Ikuta, K., Ouchi, Y., Miyazaki, J., and Shimizu, T. (1997) Role of cytosolic phospholipase A$_2$ in allergic response and parturition. *Nature* **390,** 618–622
10. Uozumi, N., and Shimizu, T. (2002) Roles for cytosolic phospholipase A$_2$α as revealed by gene-targeted mice. *Prostaglandins Other Lipid Mediat.* **68,** 59–69
11. Hirabayashi, T., Murayama, T., and Shimizu, T. (2004) Regulatory mechanism and physiological role of cytosolic phospholipase A$_2$. *Biol. Pharm. Bull.* **27,** 1168–1173
12. Perisic, O., Paterson, H. F., Mosedale, G., Lara-González, S., and Williams, R. L. (1999) Mapping the phospholipid-binding surface and translocation determinants of the C2 domain from cytosolic phospholipase A$_2$. *J. Biol. Chem.* **274,** 14979–14987
13. Stahelin, R. V., Subramanian, P., Vora, M., Cho, W., and Chalfant, C. E. (2007) Ceramide-1-phosphate binds group IVA cytosolic phospholipase A$_2$ via a novel site in the C2 domain. *J. Biol. Chem.* **282,** 20467–20474
14. Casas, J., Valdearcos, M., Pindado, J., Balsinde, J., and Balboa, M. A. (2010) The cationic cluster of group IVA phospholipase A$_2$ (Lys-488/Lys-541/Lys-543/Lys-544) is involved in translocation of the enzyme to phagosomes in human macrophages. *J. Lipid Res.* **51,** 388–399
15. Tucker, D. E., Ghosh, M., Ghomashchi, F., Loper, R., Suram, S., John, B. S., Girotti, M., Bollinger, J. G., Gelb, M. H., and Leslie, C. C. (2009) Role of phosphorylation and basic residues in the catalytic domain of cytosolic phospholipase A$_2$α in regulating interfacial kinetics and binding and cellular function. *J. Biol. Chem.* **284,** 9596–9611
16. Brown, W. J., Chambers, K., and Doody, A. (2003) Phospholipase A$_2$ (PLA$_2$) enzymes in membrane trafficking. Mediators of membrane shape and function. *Traffic* **4,** 214–221
17. Judson, B. L., and Brown, W. J. (2009) Assembly of an intact Golgi complex requires phospholipase A$_2$ (PLA$_2$) activity, membrane tubules, and dynein-mediated microtubule transport. *Biochem. Biophys. Res. Commun.* **389,** 473–477
18. San Pietro, E., Capestrano, M., Polishchuk, E. V., DiPentima, A., Trucco, A., Zizza, P., Mariggiò, S., Pulvirenti, T., Sallese, M., Tete, S., Mironov, A. A., Leslie, C. C., Corda, D., Luini, A., and Polishchuk, R. S. (2009) Group IV phospholipase A$_2$α controls the formation of inter-cisternal continuities involved in intra-Golgi transport. *PLoS Biol.* **7,** e1000194
19. Girotti, M., Evans, J. H., Burke, D., and Leslie, C. C. (2004) Cytosolic phospholipase A$_2$ translocates to forming phagosomes during phagocytosis of zymosan in macrophages. *J. Biol. Chem.* **279,** 19113–19121
20. Shmelzer, Z., Haddad, N., Admon, E., Pessach, I., Leto, T. L., Eitan-Hazan, Z., Hershfinkel, M., and Levy, R. (2003) Unique targeting of cytosolic phospholipase A$_2$ to plasma membranes mediated by the NADPH oxidase in phagocytes. *J. Cell Biol.* **162,** 683–692
21. Casas, J., Meana, C., Esquinas, E., Valdearcos, M., Pindado, J., Balsinde, J., and Balboa, M. A. (2009) Requirement of JNK-mediated phosphorylation for translocation of group IVA phospholipase A$_2$ to phagosomes in human

macrophages. *J. Immunol.* **183,** 2767–2774
22. Schievella, A. R., Regier, M. K., Smith, W. L., and Lin, L. L. (1995) Calcium-mediated translocation of cytosolic phospholipase A_2 to the nuclear envelope and endoplasmic reticulum. *J. Biol. Chem.* **270,** 30749–30754
23. Kudo, I., and Murakami, M. (2002) Phospholipase A_2 enzymes. *Prostaglandins Other Lipid Mediat.* **68,** 3–58
24. Mariggiò, S., Sebastià, J., Filippi, B. M., Iurisci, C., Volonté, C., Amadio, S., De Falco, V., Santoro, M., and Corda, D. (2006) A novel pathway of cell growth regulation mediated by a PLA$_2$α-derived phosphoinositide metabolite. *FASEB J.* **20,** 2567–2569
25. Nalefski, E. A., McDonagh, T., Somers, W., Seehra, J., Falke, J. J., and Clark, J. D. (1998) Independent folding and ligand specificity of the C2 calcium-dependent lipid binding domain of cytosolic phospholipase A_2. *J. Biol. Chem.* **273,** 1365–1372
26. Leslie, C. C. (2004) Regulation of arachidonic acid availability for eicosanoid production. *Biochem. Cell Biol.* **82,** 1–17
27. Corda, D., Iurisci, C., and Berrie, C. P. (2002) Biological activities and metabolism of the lysophosphoinositides and glycerophosphoinositols. *Biochim. Biophys. Acta* **1582,** 52–69
28. Mariggiò, S., Filippi, B. M., Iurisci, C., Dragani, L. K., De Falco, V., Santoro, M., and Corda, D. (2007) Cytosolic phospholipase A$_2$α regulates cell growth in RET/PTC-transformed thyroid cells. *Cancer Res.* **67,** 11769–11778
29. Underhill, D. M., and Ozinsky, A. (2002) Phagocytosis of microbes. Complexity in action. *Annu. Rev. Immunol.* **20,** 825–852
30. May, R. C., and Machesky, L. M. (2001) Phagocytosis and the actin cytoskeleton. *J. Cell Sci.* **114,** 1061–1077
31. Aderem, A. A., Wright, S. D., Silverstein, S. C., and Cohn, Z. A. (1985) Ligated complement receptors do not activate the arachidonic acid cascade in resident peritoneal macrophages. *J. Exp. Med.* **161,** 617–622
32. Balestrieri, B., Hsu, V. W., Gilbert, H., Leslie, C. C., Han, W. K., Bonventre, J. V., and Arm, J. P. (2006) Group V secretory phospholipase A_2 translocates to the phagosome after zymosan stimulation of mouse peritoneal macrophages and regulates phagocytosis. *J. Biol. Chem.* **281,** 6691–6698
33. Balestrieri, B., Maekawa, A., Xing, W., Gelb, M. H., Katz, H. R., and Arm, J. P. (2009) Group V secretory phospholipase A_2 modulates phagosome maturation and regulates the innate immune response against *Candida albicans*. *J. Immunol.* **182,** 4891–4898
34. Noor, S., Goldfine, H., Tucker, D. E., Suram, S., Lenz, L. L., Akira, S., Uematsu, S., Girotti, M., Bonventre, J. V., Breuel, K., Williams, D. L., and Leslie, C. C. (2008) Activation of cytosolic phospholipase Aα in resident peritoneal macrophages by *Listeria monocytogenes* involves listeriolysin O and TLR2. *J. Biol. Chem.* **283,** 4744–4755
35. Suram, S., Brown, G. D., Ghosh, M., Gordon, S., Loper, R., Taylor, P. R., Akira, S., Uematsu, S., Williams, D. L., and Leslie, C. C. (2006) Regulation of cytosolic phospholipase A_2 activation and cyclooxygenase 2 expression in macrophages by the β-glucan receptor. *J. Biol. Chem.* **281,** 5506–5514
36. Atsumi, G., Murakami, M., Kojima, K., Hadano, A., Tajima, M., and Kudo, I. (2000) Distinct roles of two intracellular phospholipase A_2s in fatty acid release in the cell death pathway. Proteolytic fragment of type IVA cytosolic phospholipase A$_2$α inhibits stimulus-induced arachidonate release, whereas that of type VI Ca^{2+}-independent phospholipase A_2 augments spontaneous fatty acid release. *J. Biol. Chem.* **275,** 18248–18258
37. Harlow, E., and Lane, D. (1988) *Antibodies: A Laboratory Manual*, Cold Spring Harbor Laboratory Press, Cold Spring Harbor, NY
38. Ono, T., Yamada, K., Chikazawa, Y., Ueno, M., Nakamoto, S., Okuno, T., and Seno, K. (2002) Characterization of a novel inhibitor of cytosolic phospholipase A$_2$α, pyrrophenone. *Biochem. J.* **363,** 727–735
39. Ghosh, M., Stewart, A., Tucker, D. E., Bonventre, J. V., Murphy, R. C., and Leslie, C. C. (2004) Role of cytosolic phospholipase A_2 in prostaglandin E_2 production by lung fibroblasts. *Am. J. Respir. Cell Mol. Biol.* **30,** 91–100
40. Brondello, J. M., Brunet, A., Pouysségur, J., and McKenzie, F. R. (1997) The dual specificity mitogen-activated protein kinase phosphatase-1 and -2 are induced by the p42/p44MAPK cascade. *J. Biol. Chem.* **272,** 1368–1376
41. Di Girolamo, M., D'Arcangelo, D., Bizzarri, C., and Corda, D. (1991) Muscarinic regulation of phospholipase A_2 and iodide fluxes in FRTL-5 thyroid cells. *Acta Endocrinol.* **125,** 192–200
42. Berrie, C. P., Iurisci, C., Piccolo, E., Bagnati, R., and Corda, D. (2007) Analysis of phosphoinositides and their aqueous metabolites. *Methods Enzymol.* **434,** 187–232
43. Absolom, D. R. (1986) Basic methods for the study of phagocytosis. *Methods Enzymol.* **132,** 95–180
44. Mosiman, V. L., Patterson, B. K., Canterero, L., and Goolsby, C. L. (1997) Reducing cellular autofluorescence in flow cytometry. An *in situ* method. *Cytometry* **30,** 151–156
45. Lehmann, A. K., Sornes, S., and Halstensen, A. (2000) Phagocytosis. Measurement by flow cytometry. *J. Immunol. Methods* **243,** 229–242
46. Stewart, C. C., Lehnert, B. E., and Steinkamp, J. A. (1986) *In vitro* and *in vivo* measurement of phagocytosis by flow cytometry. *Methods Enzymol.* **132,** 183–192
47. Larsen, E. C., Ueyama, T., Brannock, P. M., Shirai, Y., Saito, N., Larsson, C., Loegering, D., Weber, P. B., and Lennartz, M. R. (2002) A role for PKC-ϵ in FcγR-mediated phagocytosis by RAW264.7 cells. *J. Cell Biol.* **159,** 939–944
48. Pizarro-Cerdá, J., Payrastre, B., Wang, Y. J., Veiga, E., Yin, H. L., and Cossart, P. (2007) Type II phosphatidylinositol 4-kinases promote *Listeria monocytogenes* entry into target cells. *Cell. Microbiol.* **9,** 2381–2390
49. Church, W. B., Inglis, A. S., Tseng, A., Duell, R., Lei, P. W., Bryant, K. J., and Scott, K. F. (2001) A novel approach to the design of inhibitors of human secreted phospholipase A_2 based on native peptide inhibition. *J. Biol. Chem.* **276,** 33156–33164
50. Ackermann, E. J., Conde-Frieboes, K., and Dennis, E. A. (1995) Inhibition of macrophage Ca^{2+}-independent phospholipase A_2 by bromoenol lactone and trifluoromethyl ketones. *J. Biol. Chem.* **270,** 445–450
51. Dragani, L. K., Berrie, C. P., Corda, D., and Rotilio, D. (2004) Analysis of glycerophosphoinositol by liquid chromatography-electrospray ionization tandem mass spectrometry using a β-cyclodextrin-bonded column. *J. Chromatogr. B Analyt. Technol. Biomed. Life Sci.* **802,** 283–289
52. Leslie, C. C. (1997) Properties and regulation of cytosolic phospholipase A_2. *J. Biol. Chem.* **272,** 16709–16712
53. Indik, Z., Kelly, C., Chien, P., Levinson, A. I., and Schreiber, A. D. (1991) Human FcγRII, in the absence of other Fcγ receptors, mediates a phagocytic signal. *J. Clin. Invest.* **88,** 1766–1771
54. Tuijnman, W. B., Capel, P. J., and van de Winkel, J. G. (1992) Human low affinity IgG receptor FcγRIIa (CD32) introduced into mouse fibroblasts mediates phagocytosis of sensitized erythrocytes. *Blood* **79,** 1651–1656
55. Huang, Z., Payette, P., Abdullah, K., Cromlish, W. A., and Kennedy, B. P. (1996) Functional identification of the active-site nucleophile of the human 85-kDa cytosolic phospholipase A_2. *Biochemistry* **35,** 3712–3721
56. Burke, J. E., Babakhani, A., Gorfe, A. A., Kokotos, G., Li, S., Woods, V. L., Jr., McCammon, J. A., and Dennis, E. A. (2009) Location of inhibitors bound to group IVA phospholipase A_2 determined by molecular dynamics and deuterium exchange mass spectrometry. *J. Am. Chem. Soc.* **131,** 8083–8091
57. Gallop, J. L., and McMahon, H. T. (2005) BAR domains and membrane curvature. Bringing your curves to the BAR. *Biochem. Soc. Symp.* **72,** 223–231
58. Hui, E., Johnson, C. P., Yao, J., Dunning, F. M., and Chapman, E. R. (2009) Synaptotagmin-mediated bending of the target membrane is a critical step in Ca^{2+}-regulated fusion. *Cell* **138,** 709–721
59. Perisic, O., Fong, S., Lynch, D. E., Bycroft, M., and Williams, R. L. (1998) Crystal structure of a calcium-phospholipid binding domain from cytosolic phospholipase A_2. *J. Biol. Chem.* **273,** 1596–1604